RADC-TR-86-127
In-House Report
July 1986

PHASE-ONLY NULLING WITH COARSELY QUANTIZED PHASE SHIFTERS

Peter R. Franchi
Robert A. Shore

APPROVED FOR PUBLIC RELEASE; DISTRIBUTION UNLIMITED

JAN 8 1987

A

ROME AIR DEVELOPMENT CENTER
Air Force Systems Command
Griffiss Air Force Base, NY 13441-5700

AD-A175 768

DTIC FILE COPY

87   1   7   080

This report has been reviewed by the RADC Public Affairs Office (PA) and is releasable to the National Technical Information Service (NTIS). At NTIS it will be releasable to the general public, including foreign nations.

RADC-TR-86-127 has been reviewed and is approved for publication.
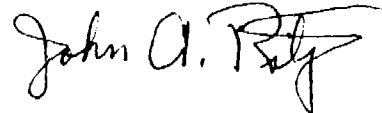
APPROVED:

J. LEON POIRIER
Chief, EM Techniques Branch
Electromagnetic Sciences Division

APPROVED:

ALLAN C. SCHELL
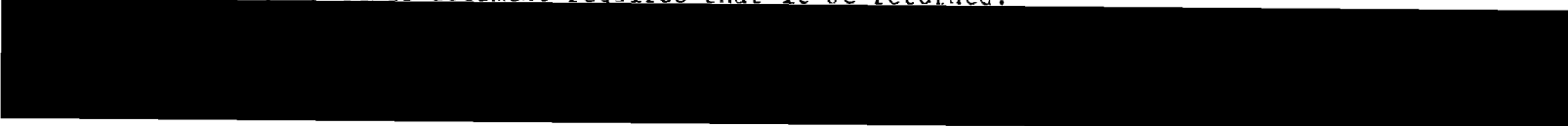Chief, Electromagnetic Sciences Division

FOR THE COMMANDER:

JOHN A. RITZ
Plans & Programs Division

REPORT DOCUMENTATION PAGE

1a. REPORT SECURITY CLASSIFICATION Unclassified		1b RESTRICTIVE MARKINGS			
2a. SECURITY CLASSIFICATION AUTHORITY		3. DISTRIBUTION / AVAILABILITY OF REPORT			
2b. DECLASSIFICATION / DOWNGRADING SCHEDULE		Approved for public release; distribution unlimited.			
4. PERFORMING ORGANIZATION REPORT NUMBER(S) RADC-TR-86-127		5. MONITORING ORGANIZATION REPORT NUMBER(S)			

6a. NAME OF PERFORMING ORGANIZATION Rome Air Development Center	6b. OFFICE SYMBOL (If applicable) EECS	7a. NAME OF MONITORING ORGANIZATION Rome Air Development Center (EECS)
6c. ADDRESS (City, State, and ZIP Code) Hanscom AFB Massachusetts 01731		7b ADDRESS (City, State, and ZIP Code) Hanscom AFB Massachusetts 01731

8a. NAME OF FUNDING / SPONSORING ORGANIZATION Rome Air Development Center	8b. OFFICE SYMBOL (If applicable) EECS	9 PROCUREMENT INSTRUMENT IDENTIFICATION NUMBER

8c. ADDRESS (City, State, and ZIP Code) Hanscom AFB Massachusetts 01731	10. SOURCE OF FUNDING NUMBERS			
	PROGRAM ELEMENT NO. 61102F	PROJECT NO. 2305	TASK NO. J3	WORK UNIT ACCESSION NO 04

11. TITLE (Include Security Classification)

Phase-Only Nulling With Coarsely Quantized Phase Shifters

12 PERSONAL AUTHOR(S) Peter R. Franchi and Robert A. Shore

13a. TYPE OF REPORT In-House	13b. TIME COVERED FROM Jan 86 TO May 86	14 DATE OF REPORT (Year, Month, Day) 1986 July	15 PAGE COUNT 30

16. SUPPLEMENTARY NOTATION

17. COSATI CODES			18. SUBJECT TERMS (Continue on reverse if necessary and identify by block number)
FIELD	GROUP	SUB-GROUP	Planar array antennas, Phase-only weight control,
0903	1709		Phase quantization, Null synthesis

19. ABSTRACT (Continue on reverse if necessary and identify by block number)

The purpose of this report is to show that deep nulls can be imposed at specified locations in planar array antenna patterns using phase-only control of coarsely quantized phase shifters. This is done by using the number of phase shifters available for control in the columns of the array to compensate for the small number of bits of the individual phase shifters. Null synthesis algorithms are derived to calculate phase shifts to impose nulls in the $\phi = 0$ pattern cut of planar array antenna patterns. Results of calculations are presented in this report.

20. DISTRIBUTION / AVAILABILITY OF ABSTRACT ☐ UNCLASSIFIED/UNLIMITED ☒ SAME AS RPT ☐ DTIC USERS	21. ABSTRACT SECURITY CLASSIFICATION Unclassified	
22a NAME OF RESPONSIBLE INDIVIDUAL Robert A. Shore	22b. TELEPHONE (Include Area Code) (617) 377-2058	22c OFFICE SYMBOL RADC/EECS

DD FORM 1473, 84 MAR

83 APR edition may be used until exhausted.
All other editions are obsolete.

Contents

Illustrations

Tables

Phase-Only Nulling With Coarsely Quantized Phase Shifters

1. INTRODUCTION

Interest in the subject of phase-only control of array antenna patterns has been stimulated by the growing importance of phased array antennas, since the required phase controls are already available as part of a beam steering system. An extensive bibliography is given in Reference 1. While from the theoretical point of view it has been established that phase-only control can be used to impose nulls at desired locations in array antenna patterns, the practicality of nulling with phase control alone has not yet been determined. Indeed there is good reason to question the practicality if costly high precision phase shifters are required to achieve deep pattern nulls.

The purpose of this report is to suggest a possible way of overcoming the limitations on depth of null that would otherwise result from using coarsely quantized phase shifters to produce pattern nulls. The basic idea is to use the number of phase shifters available for control in the columns of a planar array to compensate for the small number of bits of the individual phase shifters by averaging over the columns. In the following section of the report we describe two algorithms, one for obtaining the phase shifts to impose a single null in the $\varphi = 0°$ cut of a planar

1. Shore, R.A. (1985) A Review of Phase-Only Sidelobe Nulling Investigations at RADC, RADC-TR-85-145, AD A166602.

1

array pattern, and the second to impose multiple nulls in the $\varphi = 0°$ pattern cut. Results obtained with these algorithms are presented in Section 3 of this report. It is shown that using these methods enables deep nulls to be formed with phase shifters of even 2 bits that would otherwise require phase shifters of considerably higher precision.

2. ANALYSIS

We consider a rectangular planar array of elements with 2N columns and 2M rows. The interelement spacing of elements in the rows is denoted by d_x and that of the column elements is denoted by d_y. The field pattern of the array is given by the expression

$$p(u, v) = \sum_{n=1}^{2N} \sum_{m=1}^{2M} w_{nm} \exp[j \, (d_{x_n} u + d_{y_m} v)]$$

where

$$d_{x_n} = \frac{2N-1}{2} - (n-1), \quad n = 1, 2, \ldots, 2N$$

$$d_{y_m} = \frac{2M-1}{2} - (m-1), \quad m = 1, 2, \ldots, 2M$$

$$u = kd_x \sin(\theta) \cos(\varphi),$$

$$v = kd_y \sin(\theta) \sin(\varphi),$$

$$k = \text{wavenumber} = 2\pi/\lambda,$$

and where w_{nm} is the complex weight of the nm^{th} element. The pattern angles, θ and φ, are referred to a coordinate system with the z-axis normal to the plane of the array, and with the x- and y-axes parallel to the rows and columns respectively.

Let the unperturbed weights be denoted by $w_{onm} = a_n b_m \exp(j\varphi_{onm})$ where it is assumed that the amplitude taper can be factored into the product of a row taper and a column taper. The normalization

$$\sum_{n=1}^{2N} a_n = 1, \quad \sum_{m=1}^{2M} b_m = 1$$

2

is imposed on these tapers. The phase-only perturbed weights are then denoted by $w_{nm} = w_{onm} \exp(j\Delta\varphi_{nm})$. Throughout this report we will work exclusively with real patterns, as a condition for which we assume that the amplitude tapers are even-symmetrical

$$a_{2N-n+1} = a_n, \quad n = 1, 2, \ldots, N$$

$$b_{2M-m+1} = b_m, \quad m = 1, 2, \ldots, M$$

and the initial phases, φ_{onm}, and the phase perturbations, $\Delta\varphi_{nm}$, are odd-symmetrical

$$\varphi_{o2N-n+1,\ 2M-m+1} = -\varphi_{onm}$$

$$\Delta\varphi_{2N-n+1,\ 2M-m+1} = -\Delta\varphi_{nm} \ . \tag{1}$$

We first consider the problem of imposing a single null in the pattern at the location $u = u_1$, $v = 0$, with phase-only perturbations of the array weights; that is of obtaining a pattern with

$$\sum_n \sum_m a_n b_m \exp[j(\varphi_{onm} + \Delta\varphi_{nm} + d_{x_n} u_1)] = 0 \ . \tag{2}$$

We write Eq. (2) in the form

$$\sum_n \sum_m a_n b_m \exp[j(\varphi_{onm} + d_{x_n} u_1)]$$

$$+ \sum_n \sum_m a_n b_m \exp(j\varphi_{onm}) [\exp(j\Delta\varphi_{nm}) - 1] \exp(j d_{x_n} u_1) = 0$$

which, in view of our restriction to real patterns and the fact that the first term is the unperturbed pattern $p_o(u_1, 0)$, becomes

$$\sum_n \sum_m a_n b_m \{\sin(d_{x_n} u_1 + \varphi_{onm}) \sin \Delta\varphi_{nm}$$

$$- \cos(d_{x_n} u_1 + \varphi_{onm}) (\cos \Delta\varphi_{nm} - 1)\} = p_o(u_1, 0) \ . \tag{3}$$

3

Equation (3) can be satisfied if we can find phase perturbations such that

$$\sum_m b_m [\sin (d_{x_n} u_1 + \varphi_{onm}) \sin \Delta\varphi_{nm}$$

$$- \cos (d_{x_n} u_1 + \varphi_{onm}) (\cos \Delta\varphi_{nm} - 1)] = \frac{p_o(u_1, 0)}{2N a_n} . \qquad (4)$$

If the phase shifters are quantized with NBIT bits, then

$$\Delta\varphi_{nm} = i_{nm} B$$

where i_{nm} is an integer and $B = (2\pi)/2^{NBIT}$. Equation (4) then takes the form

$$\sum_m b_m [\sin (d_{x_n} u_1 + \varphi_{onm}) \sin (i_{nm} B)$$

$$- \cos (d_{x_n} u_1 + \varphi_{onm}) (\cos i_{nm} B - 1)] = \frac{p_o (u_1, 0)}{2N a_n} .$$

Assuming even symmetry of the phases within the columns

$$\varphi_{on, 2M-m+1} = \varphi_{onm}$$

$$\varphi_{n, 2M-m+1} = \varphi_{nm} ,$$

we obtain

$$\sum_{m=1}^{M} b_m [\sin (d_{x_n} u_1 + \varphi_{onm}) \sin (i_{nm} B)$$

$$- \cos (d_{x_n} u_1 + \varphi_{onm}) (\cos i_{nm} B - 1) = \frac{p_o (u_1, 0)}{4N a_n} . \qquad (5)$$

To determine the $\{i_{nm}\}$ we can use the following algorithm. First, since our interest is primarily in phase shifters with a small number of bits, say NBIT $\leq$ 5, and since it is desirable to keep the phase perturbations small to reduce the effect on the unperturbed pattern, we restrict the phase perturbations to be at most one bit; that is, $i_{nm} = \pm 1$ or 0. We then try to satisfy Eq. (5) by starting in the center of the column with the element with the largest amplitude factor, b_M, and working out to the edge of the column to the element with the smallest amplitude factor, b_1,

assuming a monotonically decreasing amplitude taper. Let t_{nm} denote the term of the left-hand side of Eq. (5) corresponding to the index m, and let

$$S_{nm'} = \sum_{m=M}^{m'} t_{nm}, \quad m' = M, M-1, \ldots, 1$$

$$S_{n, M+1} = 0.$$

Then we set $i_{nm'} = \pm 1$ according as the choice of sign makes $t_{nm'}$ agree in sign with that of the right-hand side of Eq. (5), and if by so doing

$$|S_{nm'}| = |S_{n, m'+1} + t_{nm'}| \le \frac{|p_o(u_1, 0)|}{4N a_n}, \quad m' = M, M-1, \ldots, 1.$$

Otherwise, we set $i_{nm'} = 0$. In other words, we attempt to satisfy Eq. (5) by summing terms of the same sign as the right-hand side, starting with the largest magnitude terms and working down to the smallest magnitude terms. The amplitude taper is essential for the algorithm to work well since the small amplitude terms at the edge of the column are used to "fine tune" the fit of the left-hand side of Eq. (5) to the right-hand side. The more pronounced the taper the closer the fit that can be made.

The efficacy of this scheme can be significantly improved upon by a simple correction technique. Let ϵ_n denote the error incurred in attempting to satisfy Eq. (5)

$$\epsilon_n = \sum_{m=1}^{M} t_{nm} - \frac{p_o(u_1, 0)}{4N a_n} = S_{n1} - \frac{p_o(u_1, 0)}{4N a_n}$$

Then the resulting error, ϵ, in satisfying Eq. (3), the condition for the pattern null at $(u_1, 0)$ is

$$\epsilon = \sum_{n=1}^{N} \epsilon_n.$$

Suppose, however, that after trying to satisfy Eq. (5) for n = 1 we then subtract the resulting error, ϵ_1, from the right-hand side of Eq. (5) for n = 2 so that the right-hand side for n = 2 becomes

$$\frac{p_o(u_1, 0)}{4N a_2} - \epsilon_1.$$

Similarly, let ϵ_2 be the error now incurred in satisfying

$$\sum_{m=1}^{M} b_m t_{2m} = \frac{p_o(u_1, 0)}{4N a_2} - \epsilon_1 .$$

We then subtract this error from the right-hand side of Eq. (5) for n = 3, and so on. The resulting total error in attempting to satisfy Eq. (3) is then

$$\epsilon = \epsilon_1 - \epsilon_1 + \epsilon_2 - \epsilon_2 + \ldots - \epsilon_{N-1} + \epsilon_N = \epsilon_N$$

so that we are left with only the error incurred in satisfying

$$\sum_{m=1}^{M} b_m t_{Nm} = \frac{p_o(u_1, 0)}{4N a_n} - \epsilon_{N-1} .$$

As will be seen in Section 3, this error correction technique results in a substantial improvement in the depth of null obtained.

The method we have discussed for producing a single pattern null with coarsely quantized phase shifters, unfortunately does not appear to be generalizable to produce multiple pattern nulls. For obtaining multiple nulls we therefore resort to a different method, namely that of finding a planar array equivalent to a linear array in the sense that for the cut v = 0, the planar array has the same pattern as a linear array with the number of elements and interelement spacing equal to the number of columns and intercolumn spacing respectively of the planar array. Let the pattern of the linear array be denoted $p_{lin}(u)$ with

$$p_{lin}(u) = \sum_{n=1}^{2N} a_n \exp[j(\Delta\varphi_n + d_n u)] = 2 \sum_{n=1}^{N} a_n \cos(\Delta\varphi_n + d_n u)$$

where

$$d_n = (2N-1)/2 - (n-1), \quad n = 1, 2, \ldots, 2N ,$$

$$u = (2\pi)/\lambda \, d \, \sin(\theta) ,$$

and the $\{\Delta\varphi_n\}$ are the phase perturbations required to impose nulls in the unperturbed pattern

$$p_o(u) = \sum_{n=1}^{2N} a_n \exp(j d_n u) = 2 \sum_{n=1}^{N} a_n \cos d_n u$$

at the locations $u = u_1, u_2, \ldots, u_K$. Method for finding the $\{\Delta\phi_n\}$ have been described in several references[1-3] and need not be discussed here. Let the planar array pattern to be made equivalent to the linear array be denoted $p_{pl}(u, 0)$ with

$$p_{pl}(u, 0) = \sum_{n=1}^{2N} a_n \sum_{m=1}^{2M} b_m \exp[j(\Delta\varphi_{nm} + d_n u)]$$

$$= \sum_{n=1}^{2N} a_n \sum_{m=1}^{2M} b_m \cos(\Delta\varphi_{nm} + d_n u)$$

$$= 2 \sum_{n=1}^{N} a_n \sum_{m=1}^{2M} b_m \cos(\Delta\varphi_{nm} + d_n u)$$

where the $\{\Delta\varphi_{nm}\}$ are the phase perturbations of the elements of the planar array to be determined. Equating $p_{pl}(u, 0)$ with $p_{lin}(u)$ then yields

$$\sum_{m=1}^{2M} b_m \cos(\Delta\varphi_{nm} + d_n u) = \cos(\Delta\varphi_n + d_n u)$$

or

$$\sum_{m=1}^{2M} b_m \cos \Delta\varphi_{nm} = \cos \Delta\varphi_n, \tag{6a}$$

$$\sum_{m=1}^{2M} b_m \sin \Delta\varphi_{nm} = \sin \Delta\varphi_n. \tag{6b}$$

In complex form, Eqs. (6a) and (6b) can be written as

$$\sum_{m=1}^{2M} b_m \exp(j \Delta\varphi_{nm}) = \exp(j \Delta\varphi_n). \tag{7}$$

As above we assume that the phase perturbations of the planar array elements are given by

$$\Delta\phi_{nm} = i_{nm} B, \quad i_{nm} = 0, \pm 1, \quad B = (2\pi)/2^{NBIT}.$$

2. Shore, R.A. (1983) Phase-Only Nulling as a Nonlinear Programming Problem, RADC-TR-83-37, AD A130552.

3. Shore, R.A. (1983) The Use of a Beam Space Representation and Nonlinear Programming in Phase-Only Nulling, RADC-TR-83-124, AD A131365.

One conclusion that can be drawn immediately from Eq. (7) is that $\sum b_m$ must be greater than one for Eq. (7) to be satisfied. For, employing a vector interpretation of Eq. (7) in the complex plane, $\exp(j\Delta\varphi_n)$ is a vector of unit magnitude directed at an angle $\Delta\varphi_n$ with the positive x-axis, while the $\{b_m \exp(ji_{nm}B)\}$ are vectors of magnitude b_m directed either along the positive x-axis or at an angle of $\pm B$ with the positive x-axis. If $\sum b_m = 1$ the resultant vector can have unit magnitude only if all the $\{i_{nm}\}$ are equal for a given value of n. Otherwise the resultant vector will have a magnitude less than one. Thus in general $\sum b_m$ must be greater than one.

Furthermore, since the resultant vector must lie in the angular sector between $-B$ and $+B$, it follows that Eq. (7) can be satisfied only for

$$|\Delta\varphi_n| \leq B .$$

This, however, is not a significant restriction for us, since our entire analysis is motivated by the problem of realizing small phase perturbations with phase shifters whose minimum quantization step is considerably larger than the desired phase perturbations. In Appendix A we derive the following expression for $\sum b_m$ as a condition for Eq. (7) to be satisfied:

$$\sum_{m=1}^{2M} b_m = \tan\frac{B}{2} \sin|\Delta\varphi_n| + \cos\Delta\varphi_n . \qquad (8)$$

Since the right-hand side of Eq. (8) varies from column to column, it follows that Eq. (7) or Eqs. (6a) and (6b) cannot be satisfied exactly if phase-only control of the array elements is employed. However it will be seen that Eqs. (6a) and (6b) can be satisfied closely enough to yield deep pattern nulls if an average value of $\sum b_m > 1$ is employed.

As a consequence of $\sum b_m > 1$, the mainbeam loss of the planar array pattern that results from imposing nulls at a set of locations $u = u_1, u_2, \ldots, u_K$ is greater than the loss incurred in the equivalent linear array pattern. For in the case of the linear array pattern the mainbeam loss incurred in imposing nulls is

$$\sum_{n=1}^{2N} a_n(1 - \cos\Delta\varphi_n) = 1 - \sum_{n=1}^{2N} a_n \cos\Delta\varphi_n$$

while for the planar array the mainbeam loss is

8

$$\sum_{n=1}^{2N} a_n \sum_{m=1}^{2M} b_m - \sum_{n=1}^{2N} a_n \sum_{m=1}^{2M} b_m \cos \Delta\varphi_{nm}$$

$$= \sum_{m=1}^{2M} b_m - \sum_{n=1}^{2N} a_n \cos \Delta\varphi_n > 1 - \sum_{n=1}^{2N} a_n \cos \Delta\varphi_n$$

The algorithm used for determining the phase shifts to satisfy Eqs. (6a) and (6b) is as follows. First the values of the $\{b_m\}$, originally normalized to sum to unity, are multiplied by a factor obtained by averaging the right-hand side of Eq. (8) over n and then adding a small constant to this average value. A two-step procedure then follows. We first try to satisfy Eq. (6b) which we write in the form

$$\sum_{m=1}^{M} b_m i_{nm} = \frac{\sin \Delta\varphi_n}{2 \sin B} \tag{9}$$

obtained from Eq. (6b) by letting $\Delta\varphi_m = i_{nm} B$, $i_{nm} = 0, \pm 1$ and using the relation

$$\sin(i_{nm} B) = i_{nm} \sin B .$$

Even symmetry of the phases with respect to the index m is assumed so that

$$i_{n, 2M-m+1} = i_{nm} . \tag{10}$$

The algorithm used for determining the $\{i_{nm}\}$ to satisfy Eq. (9) is basically the same as that described above in treating the single null problem. We let

$$S_{nm'} = \sum_{m=M}^{m'} b_m i_{nm}, \quad m' = M, M-1, \ldots, 1$$

$$S_{n, M+1} = 0 .$$

Then we set $i_{nm'} = \pm 1$ according as the choice of the sign agrees with that of $\Delta\varphi_n$ and if by so doing

$$|S_{nm'}| = |S_{n, m'+1} + b_{m'} i_{nm'}| \leq \frac{\sin |\Delta\varphi_n|}{2 \sin B}, \quad m' = M, M-1, \ldots, 1 .$$

Otherwise we set $i_{nm'} = 0$.

Having satisfied Eq. (9) as closely as possible, we then turn to Eq. (6a) which we write as

$$\sum_{m=1}^{M} b_m \cos(i_{nm} B) = \frac{\cos \Delta \rho_n}{2} .$$ (11)

The left-hand side of Eq. (11) has some value, in general not equal to the right-hand side, as a result of the settings of the $\{i_{nm}\}$ made in satisfying Eq. (9). The trick now is to adjust the $\{i_{nm}\}$ to satisfy Eq. (11) without disturbing the fit made to Eq. (9). The algorithm used to satisfy Eq. (11) without disturbing Eq. (9) changes only the values of the $\{i_{nm}\}$ left equal to zero in satisfying Eq. (9), and when a value of i_{nm} is changed from 0 to ± 1 the symmetric phase shifter in the column (index n, 2M-m+1) is changed to $-i_{nm}$ instead of being set equal to i_{nm} as when satisfying Eq. (9) [see Eq. 10)]. Thus $\sum b_m i_{nm}$ is left unchanged. Let

$$T_{n, M+1} = \sum_{m=1}^{M} b_m \cos(i_{nm} B)$$

after satisfying Eq. (9), and let

$$T_{nm'} = T_{n, M+1} + \sum_{m=M}^{m'} b_m [\cos(i_{nm} B) - 1], \quad m' = M, M-1, \ldots, 1 .$$

Then, if $i_{nm'}$ was left equal to zero after satisfying Eq. (9), we now set $i_{nm'} = \pm 1$ according as the choice of sign agrees with that of $\Delta \rho_n$ and if by so doing

$$T_{nm'} = T_{n, m'+1} + b_{m'} [\cos(i_{nm'} B) - 1] \geq \frac{\cos \Delta \rho_n}{2} .$$ (12)

Otherwise we leave $i_{nm'}$ unchanged at zero. In other words, we try to satisfy Eq. (11) from above in contrast to the procedure used to satisfy Eq. (9) which works from below. The fact that the resettings of the $\{i_{nm}\}$ to satisfy Eq. (11) result in decreasing the starting value of $T_{nm'}$, $T_{n, M+1}$, makes it important that the $\{b_m\}$ have been initially adjusted so that $T_{n, M+1}$ is larger than $\cos(\Delta \rho_n)/2$ for all n. This is done, as mentioned on page 9, by first obtaining an average multiplicative constant for the column taper by averaging the right-hand side of Eq. (8) and then adding a small term to this multiplier. As with the single null algorithm, the success of the multiple null algorithm requires a significant amplitude taper of the columns of the array since the small terms corresponding to the edge elements are used to fine tune the fit of the sums of the left-hand sides of Eqs. (6a) and (6b) to the respective right-hand sides.

3. RESULTS

In this section we present the results of calculations performed with the algorithms described in Section 2. We begin with the single-null algorithm discussed on page 4 using the error correcting scheme. In Table 1 we summarize the results obtained for a 100×100 element array by fixing the number of bits in the phase shifters and averaging the unperturbed and perturbed power at the position of the desired null, the average taken as the null position was varied from $3°$ to $15°$ at intervals of $0.2°$. The interelement spacing within the rows and columns of the array was set equal to $\lambda/2$. Row and column amplitude tapers were for a Taylor distribution with 40 dB maximum sidelobes and $\bar{n} = 4$. The phases of the unperturbed element weights were random with a uniform distribution in the interval $[-B/2, +B/2]$, $B = (2\pi)/2^{NBIT}$. The average perturbed power at the null location should be compared with the last column of the table which gives the statistical average of the power at a null location of the pattern if phase errors are uniformly distributed in the interval $[-B/2, +B/2]$. This value is computed from the formula[4]

$$\frac{\overline{|F(u,v)|^2}}{\left(\sum_n \sum_m |w_{nm}|\right)^2} = \left[1 - \left(\frac{\sin \Delta}{\Delta}\right)^2\right] \frac{\sum_n \sum_m |w_{nm}|^2}{\left(\sum_n \sum_m |w_{nm}|\right)^2}$$

with $\overline{|F(u,v)|^2}$ the statistical ensemble average power at a location in the pattern for which the error-free pattern has a null. Thus, for example, with 2-bit phase shifters the planar array is able to form nulls with an average depth of -58 dB as compared with the -40 dB nulls that could be expected if nothing were done to compensate for the small number of bits. Since the statistical average null depth decreases by approximately 6 dB for each extra phase shifter bit, the -79 dB null level obtained with 4-bit phase shifters is equivalent to that obtainable with 9-bit phase shifters if no compensating method is used.

The tapering off of the average perturbed null depth power going from 5 to 6 bits is explainable with reference to Eq. (5). As the number of bits increases, B becomes small and eventually the terms on the left-hand side become too small to match the right-hand side unless phase shifts larger than 1 bit are allowed. For 7-bit phase shifters, for example, the average perturbed power at the null location increases to -71.5 dB while for 8 bits it is only -53.6 dB.

---

4. Shore, R.A. (1982) Statistical Analysis of the Effect of Phase Quantization on Array Antenna Sidelobes, RADC-TR-82-190, AD A123704.

Table 1. Summary of Results Obtained With the Single-null Algorithm for a
100 × 100 Element Array; 40 dB, $\bar{n}$ = 4 Taylor Amplitude Tapers. Null
location varied from 3° to 15° at intervals of 0.2°

NBIT	Average Unperturbed Power (dB)	Average Perturbed Power (dB)	Reduction (dB)	Highest Pattern Value at Desired Null Location (dB)	Statistical Average Null Depth (dB)
2	-41.9	-58.0	16.1	-50.4	-40.0
3	-43.5	-69.3	25.8	-59.5	-45.1
4	-44.1	-78.8	33.7	-70.1	-50.8
5	-44.1	-88.0	43.9	-77.2	-56.8
6	-44.1	-91.8	47.7	-82.2	-62.8

The importance of the error correcting scheme discussed on page 5 becomes
apparent if one compares the results shown in Table 1 with those obtained if the
error connecting scheme is not used. For NBIT = 4 and 5, for example, without
the error correcting scheme the average power at the null location is -62.6 and
-68.9 dB respectively, contrasted with the respective values of -78.8 and -88.0 dB
obtained using the error correction scheme.

Table 2 summarizes results obtained for a 100 × 50 element array with the
same element spacing, amplitude tapers, and averaging interval as for Table 1.
An approximately 3-dB decrease in performance results from this halving of the
column size. This reduction in performance as the column size is decreased is to
be expected since the algorithm has fewer terms available as it tries to match the
left-hand side sum of Eq. (5) with the right-hand side.

Table 3 summarizes results obtained for a 100 × 100 element array with the
same parameters as for Table 1 except that a 30 dB, $\bar{n}$ = 4 Taylor distribution for
the row and column amplitude tapers is assumed. The reduction in performance
compared to Table 1 is attributable to the fact that the less pronounced amplitude
taper of the $\{b_m\}$ in Eq. (5) for the 30 dB Taylor compared to the 40 dB Taylor
distribution implies a corresponding reduction in the "fine tuning" capacity of the
algorithm in attempting to match the left-hand side sum and the right-hand side as
the edge elements of the column are approached.

Table 2. Summary of Results Obtained With the Single-null Algorithm for a
100 × 50 Element Array: 40 dB, $\bar{n}$ = 4 Taylor Amplitude Tapers. Null
location varied from 3° to 15° at intervals of 0.2°

NBIT	Average Unperturbed Power (dB)	Average Perturbed Power (dB)	Reduction (dB)	Highest Pattern Value at Desired Null Location (dB)	Statistical Average Null Depth (dB)
2	-42.1	-55.4	13.3	-46.7	-36.7
3	-43.4	-64.8	21.4	-54.3	-41.7
4	-43.6	-76.9	33.3	-67.8	-47.4
5	-44.0	-84.9	40.9	-76.3	-53.4
6	-44.1	-89.7	45.6	-80.6	-59.4

Table 3. Summary of Results Obtained With the Single-null Algorithm for a
100 × 100 Element Array; 30 dB, $\bar{n}$ = 4 Taylor Amplitude Tapers. Null
location varied from 3° to 15° at intervals of 0.2°

NBIT	Average Unperturbed Power (dB)	Average Perturbed Power (dB)	Reduction (dB)	Highest Pattern Value at Desired Null Location (dB)	Statistical Average Null Depth (dB)
2	-38.0	-56.0	18.0	-50.5	-40.9
3	-37.8	-66.1	28.3	-57.6	-45.9
4	-37.8	-74.8	37.0	-65.5	-51.6
5	-37.8	-79.6	41.8	-67.3	-57.6
6	-37.8	-80.4	42.6	-65.0	-63.6

As an example of the patterns obtained when the weights are perturbed using the single-null algorithm, Figure 1 shows the $\rho = 0°$ (v = 0) perturbed pattern with a null imposed at $\theta = 4.1°$ in the pattern of a 100 × 100 element array with half wavelength spacing, 4-bit phase shifters, and a 40 dB, $\bar{n} = 4$ Taylor amplitude distribution of the rows and columns. The unperturbed pattern is also shown for reference. The increase in sidelobe level at locations other than the null location is as high as 15 dB. Figure 2 shows the $\rho = 90°$ (u = 0) pattern for the same case. It is apparent that the perturbed pattern follows the unperturbed pattern far more closely for this cut than it does for the $\rho = 0°$ cut. The difference between the two cuts can be explained by referring to the expressions for the two pattern cuts (see Appendix B). For the $\rho = 0°$ cut,
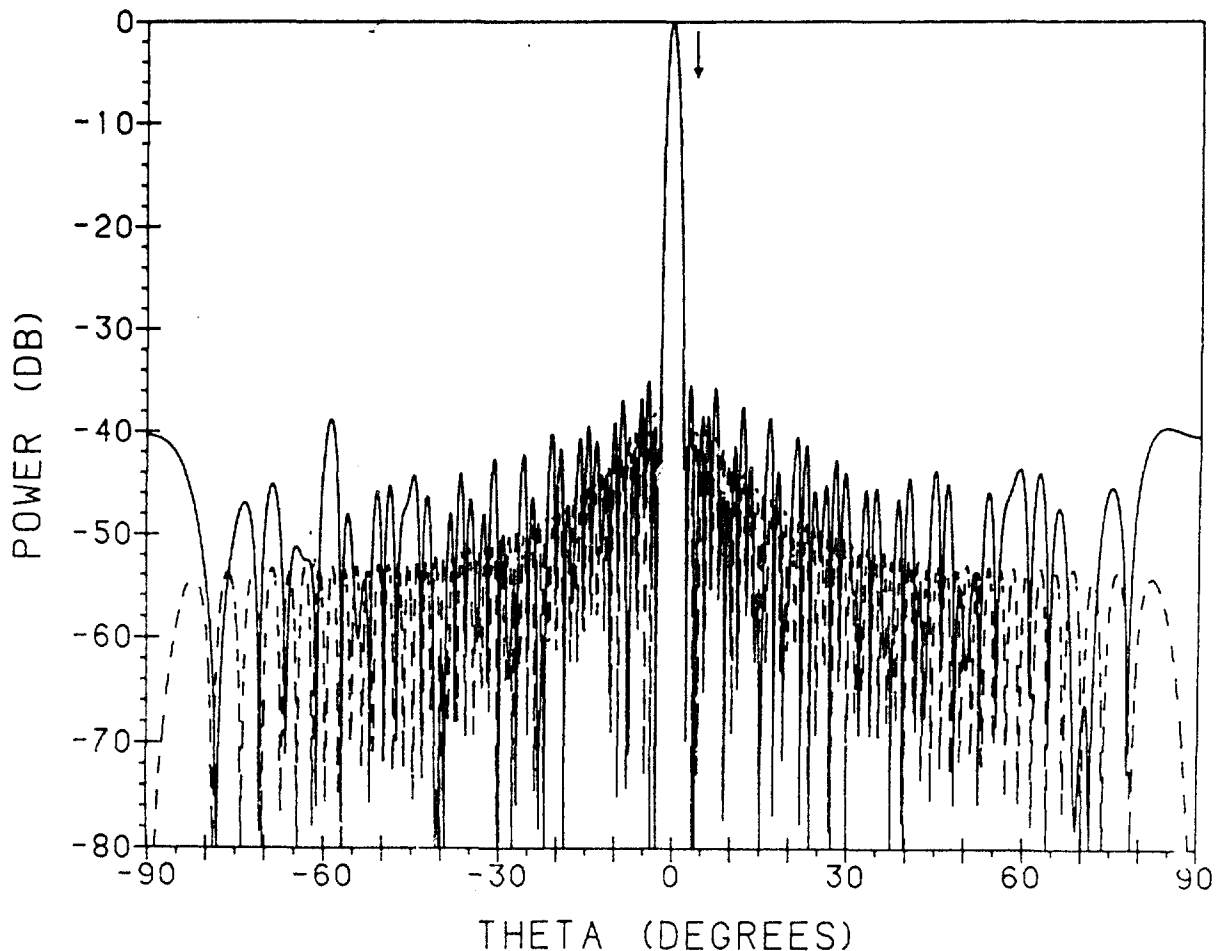

Figure 1. Unperturbed v = 0 Pattern (-----) of 100 × 100 Element Array With 40 dB, $\bar{n}$ = 4 Taylor Amplitude Tapers, and Perturbed Pattern (———) With Null Imposed at θ = 4.1° Using the Single-null Algorithm. NBIT = 4

14
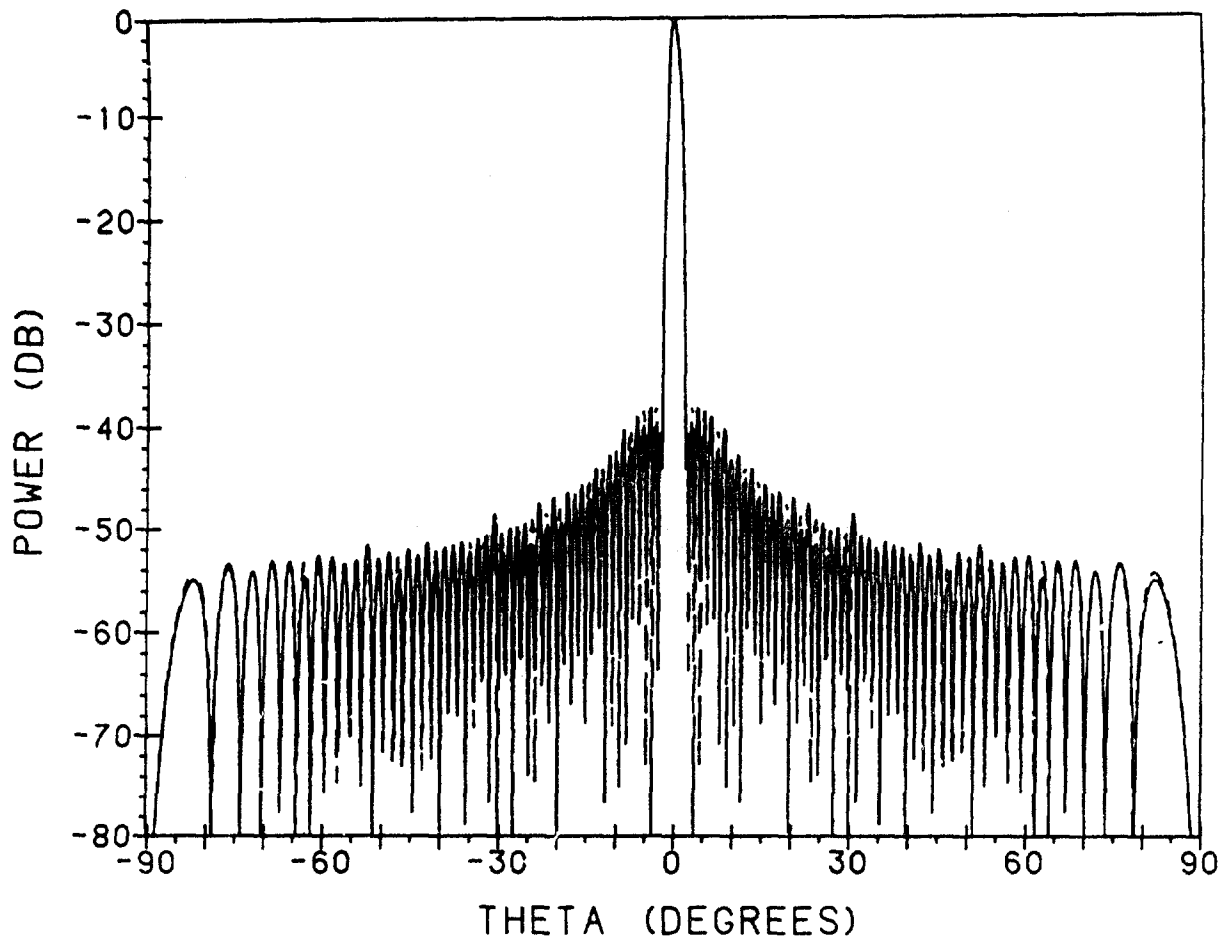
Figure 2. Unperturbed u = 0 Pattern (------) of 100 X 100 Element Array With 40 dB, $\overline{n}$ = 4 Taylor Amplitude Tapers and Perturbed Pattern (———) Corresponding to Null Imposed in the v = 0 Pattern at θ = 4.1° With the Single-null Algorithm. NBIT = 4

$$p(u, 0) = \sum_{n=1}^{2N} a_n \left\{ 2 \sum_{m=1}^{M} b_m \exp[j(\varphi_{onm} + \Delta\varphi_{nm})] \right\} \exp(jd_{x_n} u)$$

while for the $\wp$ = 90° cut

$$p(o, v) = \sum_{m=1}^{2M} b_m \left[2 \sum_{n=1}^{N} a_n \cos(\varphi_{onm} + \Delta\varphi_{nm}) \right] \exp(jd_{y_m} v) .$$

For the v = 0 pattern, the perturbed weights can be regarded as the weights, a_n, of an ideal 40 dB, $\overline{n}$ = 4 Taylor linear array multiplied by the factor

15

$$2 \sum_{m=1}^{M} b_m \exp[j(\phi_{onm} + \Delta\phi_{nm})] .$$

This factor results in a change of both amplitude and phase of the ideal Taylor weights. In contrast, for the u = 0 pattern, the perturbed weights are those of the same ideal Taylor distribution multiplied by the factor

$$2 \sum_{n=1}^{N} a_n \cos(\phi_{onm} + \Delta\phi_{nm}) .$$

This factor is real and thus modifies only the amplitude of the ideal Taylor weights. Moreover, for NBIT = 4, the argument of the cosine is for the most part less than 22.5° so that the cosine and hence the multiplicative factor itself are not very much less than unity. Thus p(0, v) does not differ significantly from the ideal Taylor pattern.

We now turn to the multiple null algorithm described on pages 9-10. Table 4 summarizes results obtained using this algorithm for the example of 5 nulls imposed in the $\phi = 0°$ (v = 0) cut of the pattern of a 100 × 100 element array with half wavelength interelement spacing at the locations $\theta = 4°$, 7°, 10°, 13°, and 16°. At these locations the unperturbed power is -40 dB, -51 dB, -44 dB, -48 dB, and -50 dB respectively. The row and column amplitude tapers are those of a 40 dB, $\bar{n} = 4$ Taylor distribution. The phase perturbations of the equivalent linear array (100 elements, half wavelength spacing, a 40 dB, $\bar{n} = 4$ Taylor amplitude taper) are those that impose nulls at the same five pattern locations while minimizing the sum of the squared weight perturbations. They were calculated using the non-linear programming method described in Reference 2. The columns of the table give respectively the number of bits in the planar array phase shifters, the depth of null achieved at the five null locations, the average power reduction, the average multiplicative constant for the column taper (obtained by averaging the expression in Eq. (8) over the columns of the array), the small term to be added to this multiplicative constant so that Eq. (12) can be satisfied (see page 10), the loss in mainbeam gain resulting from the phase perturbations (see page 9), and the statistical ensemble average null depth if nothing is done to compensate for the phase shifter quantization. The tabulated value of the small additive term was found empirically to result in the greatest average power reduction.

Table 4. Summary of Results Obtained With the Multiple-null Algorithm for a 100 × 100 Element Array: 40 dB, $\bar{n}$ = 4 Taylor Amplitude Tapers

NBIT	Perturbed Power at Null Locations (dB)					Average Unperturbed Power (dB)	Average Perturbed Power (dB)	Reduction (dB)	Average Multiplicative Factor	Additive Term	Statistical Average Null Depth (dB)	Mainbeam Gain Loss (dB)
	$\theta = 4°$	7°	10°	13°	16°							
2	-86.8	-58.1	-78.6	-64.8	-69.8	-44.2	-64.0	19.8	1.023	0.014	-40.0	0.32
3	-77.1	-68.8	-97.4	-78.4	-82.8	-44.4	-74.7	30.3	1.009	0.013	-45.1	0.19
4	-77.2	-83.5	-88.3	-84.9	-102.6	-44.4	-82.5	38.1	1.004	0.015	-50.8	0.16
5	-79.7	-95.8	-110.1	-91.0	-99.3	-44.5	-86.2	41.7	1.002	0.005	-56.8	0.06
6	-63.7	-77.4	-64.8	-72.9	-65.6	-44.6	-66.6	22.0	1.000	0.000	-62.8	0.01

17

It is apparent that remarkably deep nulls can be formed with phase shifters of even 2 bits by treating the columns of the array as single weights for a linear array and compensating for the small number of bits with the number of phase shifters available for control in the columns. As the number of bits increases, the nulling algorithm eventually breaks down, as does the single-null algorithm, because the terms of the left-hand side of Eq. (6b) become too small to match the right-hand side if phase shifts are limited to only one bit. As discussed in the previous section, in using the multiple null algorithm it is necessary to first multiply the amplitudes of the array element weights by a factor consisting of the average of Eq. (8) over the columns of the array to which is added a small term so that Eq. (12) can be satisfied by the algorithm. The average of Eq. (8) (column 10 of Table 4) decreases as the number of bits increases because $\tan(B)$ then becomes small and the average approaches the average of the cosines of the phase perturbations of the equivalent linear array. The small additive term (column 11 of Table 4) also decreases as the number of bits increases because, referring to Eq. (12), the factor $\cos(i_{nm'}B - 1)$ on the left-hand side of Eq. (12) can then decrease only very slightly if $i_{nm'}$ is changed from zero to ± 1. Hence the algorithm will be able to obtain a good match to Eq. (6a) even if the left-hand side of Eq. (12) is initially only slightly greater than the right-hand side. The mainbeam gain loss is very nearly equal to the total factor used to multiply the array weights (the sum of the average multiplicative factor and the small additive term).

To examine the effect of smaller column size on the performance of the nulling algorithm, calculations were performed with the same parameters as described above in generating Table 4 except that the column size was reduced from 100 elements to 50 and 20 elements. The results for these computations are summarized in Tables 5 and 6 respectively. It is apparent that the smaller column size reduces the ability of the algorithm to produce deep nulls at the desired locations. Nevertheless, there is still a substantial improvement even in the 20 element column case compared to the null depths that would be expected if nothing were done to compensate for the small number of bits of the phase shifters.

Table 5. Summary of Results Obtained With the Multiple-null Algorithm for a 100 × 50 Element Array: 40 dB, $\bar{n}$ = 4 Taylor Amplitude Tapers

NBIT	Perturbed Power at Null Locations (dB)					Average Unperturbed Power (dB)	Average Perturbed Power (dB)	Reduction (dB)	Average Multiplicative Factor	Additive Term	Statistical Average Null Depth (dB)	Mainbeam Gain Loss (dB)
	$\theta = 4°$	7°	10°	13°	16°							
2	-58.2	-65.5	-87.2	-76.7	-72.2	-44.3	-64.2	19.9	1.023	0.012	-36.7	0.23
3	-58.9	-77.3	-61.5	-89.8	-65.4	-44.4	-63.3	18.9	1.009	0.009	-41.7	0.16
4	-62.3	-102.8	-73.5	-80.2	-116.7	-44.4	-68.9	24.5	1.004	0.014	-47.4	0.16
5	-68.2	-98.4	-75.7	-75.9	-84.7	-44.5	-73.8	29.3	1.002	0.005	-53.4	0.15
6	-61.6	-75.1	-64.3	-70.8	-65.3	-44.6	-65.3	20.7	1.000	0.000	-59.4	0.06

Table 6. Summary of Results Obtained With the Multiple-null Algorithm for a 100 × 20 Element Array: 40 dB, $\bar{n}$ = 4 Taylor Amplitude Tapers

NBIT	Perturbed Power at Null Locations (dB)					Average Unperturbed Power (dB)	Average Perturbed Power (dB)	Reduction (dB)	Average Multiplicative Factor	Additive Term	Statistical Average Null Depth (dB)	Mainbeam Gain Loss (dB)
	$\theta = 4°$	7°	10°	13°	16°							
2	-44.7	-60.5	-50.4	-60.7	-59.6	-44.3	-50.4	6.1	1.023	0.010	-33.1	0.23
3	-50.6	-55.5	-58.6	-53.6	-64.3	-44.3	-54.5	10.2	1.009	0.015	-38.0	0.18
4	-51.4	-64.4	-61.7	-61.5	-68.8	-44.4	-57.4	13.0	1.004	0.011	-43.8	0.12
5	-56.0	-73.2	-66.6	-62.3	-70.4	-44.5	-61.6	17.1	1.002	0.004	-49.7	0.05
6	-57.3	-71.1	-64.7	-69.7	-63.1	-44.6	-62.4	17.8	1.000	0.000	-55.7	0.01

19

As an example of the patterns obtained when nulls are formed with the multiple null algorithm, Figure 3 shows the $\rho = 0°$ ($v = 0$) perturbed pattern with nulls imposed at 4°, 7°, 10°, 13°, and 16° in the pattern of a 100 × 100 element array with half wavelength spacing, 4-bit phase shifters, and a 40 dB, $\bar{n} = 4$ Taylor amplitude distribution of the rows and columns. The perturbed pattern follows the unperturbed pattern extremely closely except in the vicinity of the null locations and the locations symmetric to the nulls with respect to the mainbeam. This is very close to the typical error free pattern of a linear array with nulls imposed using minimum weight perturbation, phase-only nulling, which, of course, is what the multiple null algorithm was designed to accomplish.
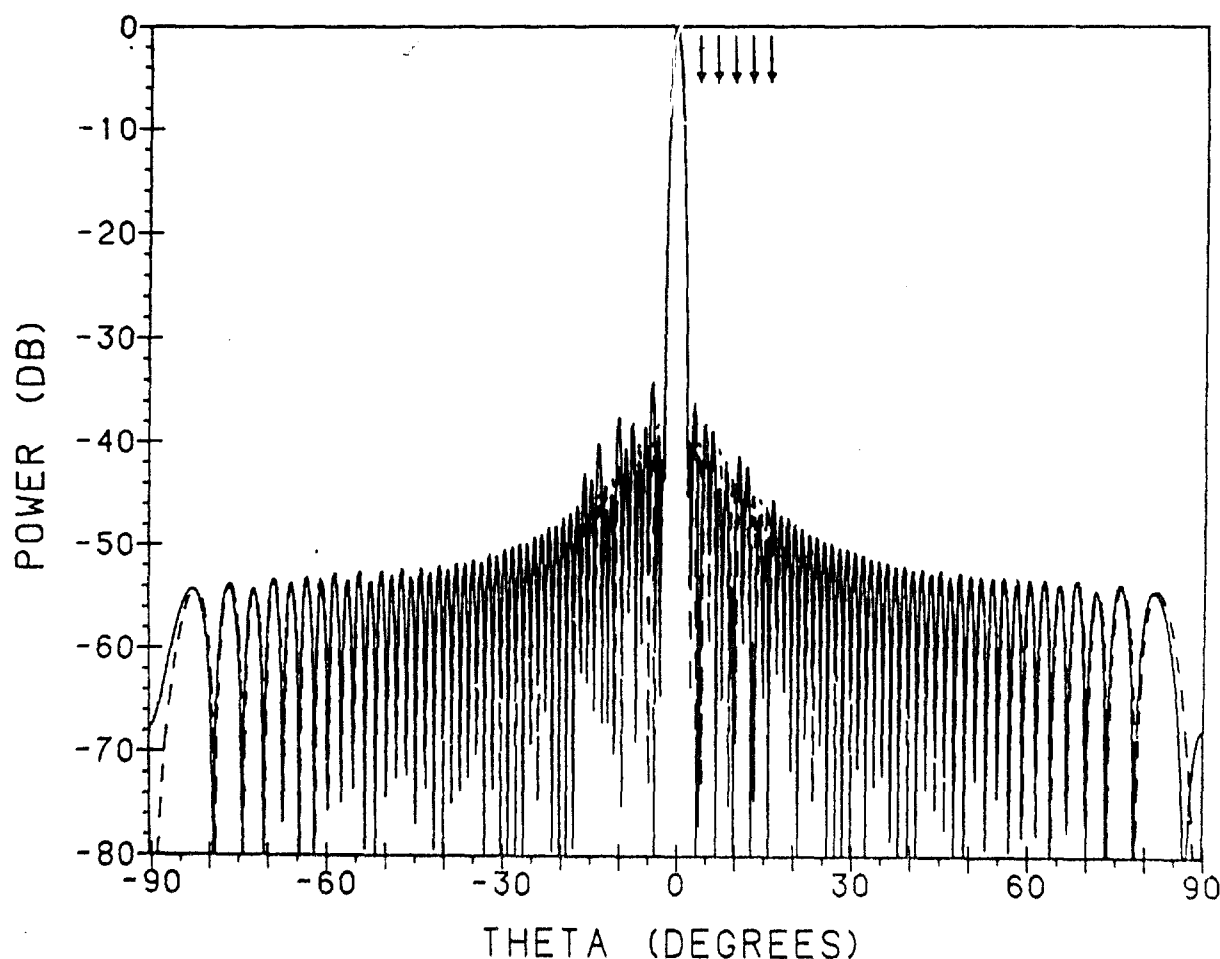

Figure 3. Unperturbed $v = 0$ Pattern (-----) of 100 × 100 Element Array With 40 dB, $\bar{n} = 4$ Taylor Amplitude Tapers, and Perturbed Pattern (————) With Nulls Imposed at $\theta = 4°$, 7°, 10°, 13°, and 16° Using the Multiple Null Algorithm. NBIT = 4

Figure 4 shows the φ = 90° (u ≈ 0) pattern for the same case (for the expressions for the principal cut patterns, see Appendix B). As might be expected, the perturbed u = 0 pattern shows significant differences from the unperturbed pattern throughout the range of θ, simply because the algorithm we have used is concerned solely with matching the v = 0 pattern cut with a given pattern of a linear array, and does not contain any safeguards for the integrity of the u = 0 pattern.
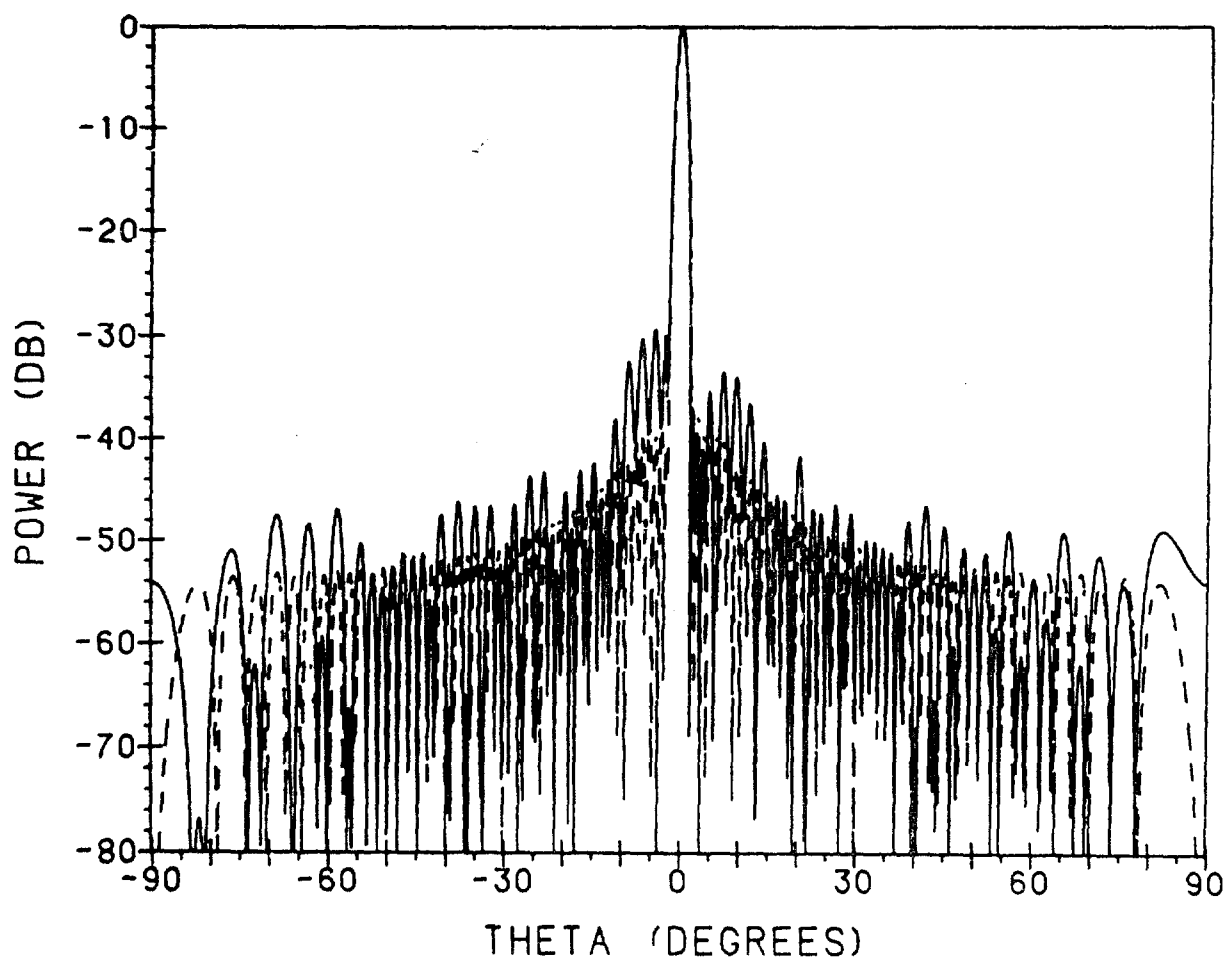

Figure 4. Unperturbed u = 0 Pattern (-----) of 100 × 100 Element Array With 40 dB, n̄ = 4 Taylor Amplitude Tapers, and Perturbed Pattern (————) Corresponding to Nulls Imposed in the v = 0 Pattern at θ = 4°, 7°, 10°, 13°, and 16° With the Multiple Null Algorithm.   NBIT = 4

4. DIRECTIONS FOR FURTHER RESEARCH

The principal purpose of this report has been to demonstrate the feasibility of obtaining deep nulls in planar array antenna patterns using coarsely quantized phase shifters. For the sake of simplicity we limited our discussion to nulls imposed in the $v = 0$ cut of real planar array antenna patterns, and developed null synthesis algorithms to obtain phase shifts for these situations. In future work we intend to consider the use of coarsely quantized phase shifters to impose nulls in arbitrary directions in both real and complex antenna patterns. Also to be considered is the possibility of using phase-only nulling with coarsely quantized phase shifters in planar arrays to accomplish what can only be done with combined amplitude and phase control in linear arrays. An example is the imposing of nulls at pattern locations symmetric with respect to the mainbeam in real linear array patterns, when the phase perturbations are not allowed to be large. Finally, since this report has considered null synthesis only, it is of much importance to investigate adaptive nulling procedures using coarsely quantized phase shifters in planar arrays.

The starting point for the derivation is Eqs. (6a) and (6b) with $\Delta\varphi_{nm} = i_{nm}B$, $B = (2\pi)/2^{NBIT}$, $i_{nm} = 0, \pm 1$:

$$\sum_{m=1}^{2M} b_m \cos(i_{nm}B) = \cos \Delta\phi_n , \tag{A1a}$$

$$\sum_{m=1}^{2M} b_m \sin(i_{nm}B) \quad \sin \Delta\phi_n . \tag{A1b}$$

Expanding Eq. (A1a),

$$\sum_m b_m \left(1 - i_{nm}^2 \frac{B^2}{2!} + i_{nm}^4 \frac{B^4}{4!} - + \ldots\right) = \cos \Delta\phi_n$$

and since $i_{nm}^{2p} = |i_{nm}|$,

$$\sum_m b_m - \sum_m b_m |i_{nm}| \left(\frac{B^2}{2!} - \frac{B^4}{4!} + - \ldots\right) = \cos \Delta\phi_n$$

or

$$\sum_{m} b_{m} = \sum_{m} b_{m} \left| i_{nm} \right| (1 - \cos B) + \cos \Delta \varphi_{n} \, . \qquad \text{(A1c)}$$

Since $\sin(i_{nm} B) = i_{nm} \sin(B)$, Eq. (A1b) can be written

$$\sum_{m} b_{m} i_{nm} = \frac{\sin \Delta \phi_{n}}{\sin B}$$

and furthermore, since the multiple null algorithm sets the sign of the $\left\{ i_{nm} \right\}$ to agree with that of $\Delta \phi_{n}$,

$$\sum_{m} b_{m} \left| i_{nm} \right| = \frac{\sin \left| \Delta \phi_{n} \right|}{\sin B} \, . \qquad \text{(A1d)}$$

Substituting Eq. (A1d) in Eq. (A1c) we obtain

$$\sum_{m} b_{m} = \frac{1 - \cos B}{\sin B} \sin \left| \Delta \phi_{n} \right| + \cos \Delta \varphi_{n}$$

$$= \tan \frac{B}{2} \sin \left| \Delta \phi_{n} \right| + \cos \Delta \varphi_{n} \, .$$

Appendix B

Expressions for the Principal Plane Patterns

In this appendix we derive expressions for the $u = 0$ and $v = 0$ patterns obtained using the single-null and multiple-null algorithms. In general, letting ϕ_{nm} denote the perturbed phases, the perturbed pattern is given by

$$p(u, v) = \sum_{n=1}^{2N} \sum_{m=1}^{2M} a_n b_m \exp(j\phi_{nm}) \exp[j (d_{x_n} u + d_{y_m} v)]$$

so that

$$p(u, 0) = \sum_{n=1}^{2N} a_n \left[\sum_{m=1}^{2M} b_m \exp(j\phi_{nm}) \right] \exp(j d_{x_n} u) \qquad \text{(B1a)}$$

and

$$p(0, v) = \sum_{m=1}^{2M} b_m \left[\sum_{n=1}^{2N} a_n \exp(j\phi_{nm}) \right] \exp(j d_{y_m} v) . \qquad \text{(B1b)}$$

For the single-null algorithm

$$\phi_{n, 2M - m + 1} = \phi_{nm} \qquad \text{(B2)}$$

so that

$$p(u, 0) = \sum_{n=1}^{2N} a_n \left[2 \sum_{m=1}^{M} b_m \exp(j\phi_{nm}) \right] \exp(jd_{x_n} u) . \tag{B3}$$

Equation (B1b) then coupled with the general symmetry relation Eq. (1) and Eq. (B2) gives

$$p(0, v) = \sum_{m=1}^{2M} b_m \left(2 \sum_{n=1}^{N} a_n \cos \phi_{nm} \right) \exp(jd_{y_m} v). \tag{B4}$$

For the multiple-null algorithm, some of the phases satisfy Eq. (B2), while others instead satisfy

$$\phi_{n, 2M - m + 1} = - \phi_{nm} .$$

Hence the simpler forms, Eqs. (B3) and (B4) obtained for the single-null case, do not apply and the general forms, Eqs. (B1a) and (B1b) must be used to calculate the patterns.

MISSION
of
Rome Air Development Center

RADC plans and executes research, development, test and selected acquisition programs in support of Command, Control, Communications and Intelligence (C^3I) activities. Technical and engineering support within areas of competence is provided to ESD Program Offices (POs) and other ESD elements to perform effective acquisition of C^3I systems. The areas of technical competence include communications, command and control, battle management, information processing, surveillance sensors, intelligence data collection and handling, solid state sciences, electromagnetics, and propagation, and electronic, maintainability, and compatibility.